Active Caspases and Cleaved Cytokeratins Are Sequestered into Cytoplasmic Inclusions in TRAIL-induced Apoptosis

Marion MacFarlane, Wendy Merrison, David Dinsdale, and Gerald M. Cohen

Medical Research Council Toxicology Unit, University of Leicester, Leicester LE1 9HN, United Kingdom

Abstract. Tumor necrosis factor–related apoptosis-inducing ligand (TRAIL) –induced apoptosis, in transformed human breast epithelial MCF-7 cells, resulted in a time-dependent activation of the initiator caspases-8 and -9 and the effector caspase-7. Cleavage of caspase-8 and its preferred substrate, Bid, preceded processing of caspases-7 and -9, indicating that caspase-8 is the apical initiator caspase in TRAIL-induced apoptosis. Using transient transfection of COOH-terminal–tagged green fluorescent protein fusion constructs, caspases-3, -7, and -8 were localized throughout the cytoplasm of MCF-7 cells. TRAIL-induced apoptosis resulted in activation of caspases-3 and -7, and the redistribution of most of their detectable catalytically active small subunits into large spheroidal cytoplasmic inclusions, which lacked a limiting membrane. These inclusions, which were also induced in untransfected cells, contained cytokeratins 8, 18, and 19, together with both a phosphorylated form and a caspase-cleavage fragment of cytokeratin 18. Similarly, in untransfected breast HBL100 and lung A549 epithelial cells, TRAIL induced the formation of cytoplasmic inclusions that contained cleaved cytokeratin 18 and colocalized with active endogenous caspase-3. We propose that effector caspase-mediated cleavage of cytokeratins, resulting in disassembly of the cytoskeleton and formation of cytoplasmic inclusions, may be a characteristic feature of epithelial cell apoptosis.

Key words: Bid • caspase immunolocalization • epithelial cells • intermediate filaments • K18

Introduction

Apoptosis is a process of fundamental importance to multicellular organisms that enables control of cell populations and the removal of damaged or potentially harmful cells (Arends and Wyllie, 1991). Apoptosis occurs in two phases: an initial commitment phase followed by an execution phase involving cytoskeletal disruption, membrane blebbing, condensation and fragmentation of chromatin, and the formation of apoptotic bodies (Earnshaw, 1995). Caspases, a family of aspartate-specific cysteine proteases, play a critical role in the execution phase of apoptosis and are the key effectors responsible for many of the dramatic morphological and biochemical changes of apoptosis (for reviews see Cohen, 1997; Thornberry and Lazebnik, 1998). Caspases are proteolytically cleaved at specific aspartate residues, generating a large and small subunit that together form the active enzyme. Caspases can be divided into two classes: (1) initiator caspases, with long prodomains, such as caspases-8 and -9, which either directly or indirectly activate (2) effector caspases, such as caspases-3, -6, and -7 (Srinivasula et al., 1996; Cohen, 1997; Thornberry and Lazebnik, 1998). During the execution phase of apoptosis, active effector caspases cleave intracellular substrates including poly(ADP-ribose) polymerase (Lazebnik et al., 1994) and the cytoskeletal components actin (Kayalar et al., 1996) and lamins (Takahashi et al., 1996).

Caspase-mediated proteolytic cleavage of lamins facilitates nuclear collapse, which is so widely used to distinguish apoptotic cells (Rao et al., 1996). More recently, it has been reported that several type I and type II intermediate filament proteins, which comprise the acidic (K9–K20) and basic cytokeratins (K1–K8) are dramatically reorganized in cells during apoptosis (Caulin et al., 1997). Cytokeratin 8 (K8)[1] and cytokeratin 18 (K18) are the major components of intermediate filaments in simple or sin-

Address correspondence to Dr. G.M. Cohen, Medical Research Council Toxicology Unit, Hodgkin Building, University of Leicester, P.O. Box 138, Lancaster Road, Leicester LE1 9HN, United Kingdom. Tel.: 44-116-2525544. Fax: 44-116-2525616. E-mail: gmc2@le.ac.uk

[1]*Abbreviations used in this paper:* GFP, green fluorescent protein; K8, K18, and K19, cytokeratins 8, 18, and 19, respectively; TNF, tumor necrosis factor; TRAIL, tumor necrosis factor-related apoptosis-inducing ligand; YVAD.CMK, acetyl-Tyr-Val-Ala-Asp chloromethyl ketone; z-DEVD.AFC, benzyloxycarbonyl-Asp-Glu-Val-Asp aminofluoromethyl coumarin; z-VAD.FMK, benzyloxycarbonyl-Val-Ala-Asp-(OMe) fluoromethyl ketone.

gle layer epithelial tissues (Moll et al., 1982). Both K8 and K18 are subject to posttranslational modification by phosphorylation (Ku and Omary, 1994). The reorganization of K8/K18 filaments during apoptosis is associated with the phosphorylation of K18 on serine 53 (previously referred to as serine 52 relative to posttranslational processed protein; Ku and Omary, 1994). Furthermore, K18 is cleaved in vitro by recombinant caspases, and such cleavage may initiate the orderly processing of filament proteins during apoptosis (Caulin et al., 1997).

Triggering of the CD95 (Fas/APO-1) receptor with its cognate ligand or agonistic antibody results in receptor trimerization and recruitment of FADD/MORT1, which in turn binds to the death effector domains of caspase-8, resulting in its activation (Boldin et al., 1996; Muzio et al., 1996). As caspase-8 activates all known caspases in vitro (Srinivasula et al., 1996), it is a prime candidate for an initiator caspase in many other forms of receptor-mediated apoptosis. Mitochondria also have been proposed to act as an amplifier in CD95-induced apoptosis with their involvement being more important in certain cell types (Kuwana et al., 1998; Scaffidi et al., 1998). Bid, a BH3 domain-containing proapoptotic Bcl-2 family member, is a cytosolic substrate of caspase-8, which when cleaved, translocates to the mitochondria where it induces the release of cytochrome *c* (Wang et al., 1996; Li et al., 1998; Luo et al., 1998). In the presence of cytochrome *c*, dATP, and Apaf-1, procaspase-9 can act as an initiator caspase, leading to the activation of the downstream effector caspases-3, -6, and -7 (P. Li et al., 1997). It remains to be determined whether this mitochondrial amplification loop, activated after CD95 receptor engagement, is also involved in other forms of receptor-mediated apoptosis.

Tumor necrosis factor–related apoptosis-inducing ligand (TRAIL), like CD95, is a member of the tumor necrosis factor (TNF) ligand family and induces apoptosis by binding to the receptors TR-1 (also called DR4) and TR-2 (also called DR5/TRICK-2/KILLER; for review see Ashkenazi and Dixit, 1998). Induction of apoptosis via this pathway is thought to be mediated through caspase activation, although the caspases involved or their order of activation in intact cells has not been demonstrated clearly. Regulation of TRAIL-induced apoptosis is, in part, controlled by the relative levels of the death receptors TR-1 and TR-2 and the decoy receptors TR-3 (also called TRID/DcR1/LIT) and TR-4 (also called DcR2/TRUNDD; Ashkenazi and Dixit, 1998). Specifically, expression of the decoy receptors in cell lines correlates, in some instances, with resistance to TRAIL-induced apoptosis (Pan et al., 1997; Sheridan et al., 1997); thus, their relative levels may contribute to the reported selective cytotoxic potential of TRAIL in some tumors (Walczak et al., 1999).

We, and others, have recently shown that distinct caspase cascades are initiated during CD95-induced apoptosis (Scaffidi et al., 1998; Sun et al., 1999). We now demonstrate that during TRAIL-induced apoptosis in MCF-7 cells, the initiator caspase-8 is activated at the apex of a caspase cascade. Apoptosis induced in MCF-7, breast HBL100 and lung A549 epithelial cells results in the formation of spheroidal cytoplasmic inclusions. In HBL100 and A549 cells, these inclusions contain cleaved cytokeratins, which colocalize with active endogenous caspase-3. Thus, sequestration of active effector caspases together with cleaved cytokeratins in epithelial cells undergoing apoptosis may facilitate the ordered dismantling of the filament network in epithelial cells during the execution phase of apoptosis.

Materials and Methods

Materials

Media and serum were purchased from Life Technologies, Inc. The caspase inhibitor, benzyloxycarbonyl-Val-Ala-Asp (OMe) fluoromethyl ketone (z-VAD.FMK) and the caspase-3 substrate, benzyloxycarbonyl-Asp-Glu-Val-Asp aminofluoromethyl coumarin (z-DEVD.AFC) were purchased from Enzyme Systems Inc., and acetyl-Tyr-Val-Ala-Asp chloromethyl ketone (YVAD.CMK) was purchased from Bachem. Anti-CD95 mAb was obtained from Upstate Biotechnology Inc. The fluorescent probe MitoTracker™ red CMXRos was purchased from Molecular Probes, Inc. All other chemicals and antibodies, unless stated otherwise, were obtained from Sigma-Aldrich.

Generation of Expression Constructs

Full-length caspases-3 and -7, and caspase-8 C345A were synthesized by PCR amplification and cloned into the pEGFP-N1 expression vector (CLONTECH Laboratories, Inc.). The caspase-8 C345A encodes a protein with a cysteine to alanine mutation at its active site to partially inhibit the cell killing induced by autoprocessing of exogenously expressed caspase-8. PCR was performed using Expand™ High Fidelity (Boehringer Mannheim) to minimize errors, and the products were purified and digested with restriction enzymes (GIBCO BRL, Life Technologies, Inc.). PCR primers were designed so that a restriction enzyme site was introduced before the start and stop codons with GFP tagged in-frame at the COOH terminus of the expressed caspase. The fragments were ligated into the BamHI and XhoI sites (caspases-3 and -7), or the HindIII and XhoI sites (caspase-8) of pEGFP-N1 and all constructs were confirmed by sequencing.

Cell Culture, Transient Transfection, and Quantification of Apoptosis

MCF-7-Fas (MCF-7) human breast epithelial cells (provided by Dr. M Jattella, Danish Cancer Society Research Center, Copenhagen, Denmark) were grown in RPMI 1640 supplemented with 10% FBS and 2 mM Glutamax™. HBL100 human breast epithelial cells and A549 human lung type II pneumocytes (both obtained from European Collection of Animal Cell Cultures) were grown in DME supplemented with 10% FBS. The cells were cultured in an atmosphere of 5% CO_2 in air at 37°C and maintained in logarithmic growth phase by routine passage every 3–4 d. Cells were plated at a density of 2×10^5 cells per well in 6-well dishes and 2 d later, were transiently transfected either using Lipofectamine (GIBCO BRL) or Fujene™ 6 (Boehringer Mannheim) according to the manufacturer's instructions, using between 2 and 4 μg DNA for each transfection. Where indicated, cells were treated at the time of transfection with z-VAD.FMK (10–50 μM) or YVAD.CMK (10–50 μM). At 16–24 h after transfection, cells were treated with 1 μg/ml recombinant soluble TRAIL (MacFarlane et al., 1997a) or 100 ng/ml anti-CD95 for the indicated times and apoptosis quantified by phosphatidylserine exposure using Annexin V-PE (PharMingen). MCF-7 cell lysates were prepared as described previously (MacFarlane et al., 1997b) and activated by the addition of 2 mM dATP, 0.25 mg/ml cytochrome *c*, and 2 mM $MgCl_2$. The proteolytic activity (cleavage of z-DEVD.AFC) of the lysate was measured as described previously (MacFarlane et al., 1997b).

Cell Sorting

MCF-7 cells were transfected with EGFP-tagged caspase-7 and, 48 h after transfection, the cells were treated with 1 μg/ml TRAIL for 5 h at 37°C. The medium was removed and spun down at 200 *g* for 3 min at 4°C to collect any apoptotic cells that had become detached from the plate. The remaining attached cells were collected by trypsinization and the detached and adherent cells were pooled, spun down, washed in ice-cold PBS, and resuspended in 5 ml ice-cold PBS. The cells were sorted on a FACS® Van-

tage (Becton Dickinson), and populations of cells exhibiting low or high intensity green fluorescence were collected for analysis by Western blotting.

Gel Electrophoresis and Immunoblotting

Equal numbers of cells were lysed in SDS-PAGE buffer and separated on 10% (GFP, K8, and K19) or 12% (caspases, Bid, and K18) SDS-polyacrylamide gels, followed by electrophoretic transfer onto nitrocellulose (Hybond-C extra; Amersham) as previously described (MacFarlane et al., 1997b). Equal protein loading per lane was verified by staining the membranes with 0.1% Ponceau S. Immunodetection was carried out using the enhanced chemiluminescence detection system (Amersham) according to the manufacturer's instructions.

Primary Antibodies

Antibodies to caspase-3 (from Dr. D. Nicholson, Merck Frosst, Quebec, Canada), caspases-7, -8, and -9 (provided by Dr. D. Green, Institute for Allergy and Immunology, La Jolla, CA), and Bid (from Dr. X. Wang, University of Texas Southwestern Medical Center, Dallas, TX) were used for Western blot analysis, as previously described (Sun et al., 1999). The rabbit polyclonal antibody CM1, specific for the p18 subunit of activated caspase-3 (Srinivasan et al., 1998; provided by IDUN, La Jolla, CA), was used at a 1:2,500 dilution for fluorescence immunocytochemistry. The rabbit polyclonal antibody to GFP was obtained from CLONTECH Laboratories, Inc., and used at a 1:2,000 dilution for immunoblotting. The mouse mAb M20, specific for K8, and A53-B/A2, specific for K19, were both used at a 1:10,000 dilution for Western blotting, at 1:250 for fluorescence immunocytochemistry and at 1:5–1:100 for ultrastructural immunocytochemistry. The 3055 rabbit polyclonal antibody, specific for K18 phosphorylated on serine 53 (Liao et al., 1995; provided by Dr. B. Omary, Stanford University School of Medicine, Stanford, CA), was used at 1:10,000 for immunoblotting, at 1:250 for fluorescence immunocytochemistry, and at 1:100 for ultrastructural immunocytochemistry. The CY-90 mouse mAb, specific for K18, was used at a 1:20,000 dilution for immunoblotting, 1:500 for fluorescence immunocytochemistry, and 1:200 for ultrastructural immunocytochemistry. The mouse mAb, M30 (Boehringer Mannheim), which specifically detects a caspase cleavage site in K18 at $DALD^{397}\downarrow S$ (Leers et al., 1999), was used at 1:200 for fluorescence immunocytochemistry and at 1:100 for ultrastructural immunocytochemistry. The M30 antibody specifically labels apoptotic epithelial cells and does not label viable or necrotic cells (Leers et al., 1999). The calnexin antibody, clone calnexin-CT (Stressgen Biotechnology Corp.), was used at a dilution of 1:100 for fluorescence immunocytochemistry. The mAbs, clone 6-11B-1, to acetylated tubulin, clone AC15, specific for β-actin and clone Vim3B4, to vimentin (Boehringer Mannheim) were also used.

Immunofluorescence Microscopy

Cells were grown on coverslips and, where indicated, MCF-7 cells were transfected as described. Before nuclear staining, the cells were washed three times with PBS and fixed in 4% paraformaldehyde for 10 min at room temperature. Coverslips were rinsed three times with PBS and stained for 10 min with 0.5 μg/ ml propidium iodide and 0.2 mg/ml RNase A, followed by a final rinse in PBS and mounting. Staining of the mitochondria was performed by incubating cells with MitoTracker™ red CMXRos (20 nM) for 15 min at 37°C. The cells were washed twice in PBS, fixed for 10 min in 4% paraformaldehyde, and mounted. For immunocytochemistry, the cells were fixed in methanol/acetone (1:1) for 20 min, permeabilized using 0.1% Triton in PBS for 30 min, and rinsed twice in PBS. After blocking in PBS containing 4% BSA for 1 h, the cells were incubated with primary antibody and diluted in 4% BSA for 2–4 h at room temperature. The cells were rinsed twice with PBS and left for 30 min in PBS before adding the secondary antibody for 1 h at 37°C. These secondary antibodies, anti-mouse or anti-rabbit Alexa 568 and 488 (Molecular Probes Inc.), respectively, were used at 1:200 dilution. The cells were washed and, where indicated, nuclei were labeled by staining cells for 20 min with Hoechst 33258 (5 μg/ml) or propidium iodide (0.5 μg/ml) before mounting onto glass slides using Vectashield® (Vector Laboratories). Optical sections were taken using an argon-krypton laser and a Leica TCS-4D confocal imaging system.

Electron Microscopy and Immunogold Cytochemistry

Nonadherent cells were dislodged by swirling the medium before removal, and spun down in a swing-out rotor at 3,000 *g*. The pellets, like the cells remaining in the plates, were fixed overnight, at 4°C, with 2% glutaraldehyde in 0.1 M sodium cacodylate buffer, pH 7.4. Adherent cells were processed in situ or scraped from the plates and spun down to form pellets. All samples were postfixed with 1% osmium tetroxide/1% potassium ferrocyanide, en bloc stained with 5% uranyl acetate, and embedded in Taab epoxy resin (Taab Ltd.). Duplicate pellets were fixed with a mixture of 4% formaldehyde, freshly made from paraformaldehyde, and 0.1% glutaraldehyde in Dulbecco's PBS, pH 7.4, for 1 h at room temperature. They were rinsed in PBS and embedded in Unicryl resin (Dinsdale et al., 1999). Ultrathin sections were blocked with normal goat serum, diluted 1:50 in PBS containing 1% BSA and 1% Tween 20, for 4 h at room temperature. Serial sections were incubated, for 18 h at 4°C, with antibodies to β-actin, tubulin, vimentin, and a range of cytokeratins. These primary antibodies were all diluted in PBS containing 1% normal goat serum, 1% BSA, and 1% Tween 20 (PBSGAT). In control incubations, the primary antibodies were replaced with mouse IgG1 or normal rabbit serum (Dako Ltd). Thorough washing in PBSGAT was followed by incubation, for 18 h at 4°C, in the appropriate goat-derived anti–mouse or anti–rabbit IgG (British Biocell International Ltd). These secondary antibodies, which had been absorbed against human serum proteins and conjugated with 10 nm colloidal gold, were diluted 1:50 in PBSGAT. Sections incubated with a mixture of the M30 and 3055 antibodies were subsequently labeled with a mixture of anti-mouse antibody conjugated with 10 nm gold and anti-rabbit antibody conjugated with 5 nm gold, respectively. Ultrathin sections were examined unstained or after staining with lead citrate and/or uranyl acetate.

Results

TRAIL-induced Apoptosis in MCF-7 Cells Results in an Early Activation of the Initiator Caspase-8 and Its Obligatory Substrate Bid

TRAIL induced a time-dependent induction of apoptosis in MCF-7 cells when assessed, by determining the percentage of apoptotic nuclei with ~35% apoptosis detected by 6 h. To determine which caspases were activated and their order of activation, Western blot analysis was performed. In untreated MCF-7 cells, caspase-8 was present primarily as two isoforms of ~55 kD (Fig. 1 A, lane 1), corresponding to caspase-8a and -8b (Scaffidi et al., 1997). Induction of apoptosis by TRAIL resulted in a time-dependent processing of caspase-8 initially to two fragments of ~43 and 41 kD, corresponding to cleavage of the small subunit from caspase-8a and -8b. This was followed by the appearance of a p18 subunit as a result of cleavage of the death effector domains from the 43- and 41-kD fragments (Fig. 1 A, lanes 2–7). An increase in the processing of caspase-8 (to yield fragments of 41 and 43 kD) was first observed 30 min after TRAIL treatment. Untreated MCF-7 cells contained the 46-kD proform of caspase-9 (Fig. 1 A, lane 1), which on induction of apoptosis by TRAIL, was processed in a time-dependent manner to yield fragments of 37 and 35 kD (Fig. 1 A, lanes 2–7), as a result of cleavage at Asp 315 and Asp 330 (Srinivasula et al., 1998). Caspase-7, a major effector caspase, was present in MCF-7 cells primarily as its intact 35-kD proform (Fig. 1 A, lane 1). Treatment with TRAIL resulted in a time-dependent processing of caspase-7, which was accompanied by the formation of the 19-kD catalytically active large subunit (Fig. 1 A, lanes 2–7). Processing of caspases-7 and -9 was first observed 60–120 min after treatment with TRAIL.

Bid is a specific proximal substrate of caspase-8 in the CD95 signaling pathway (Li et al., 1998; Luo et al., 1998). Cleavage of Bid by caspase-8 realizes its potent proapoptotic activity, which is important for the release of cyto-

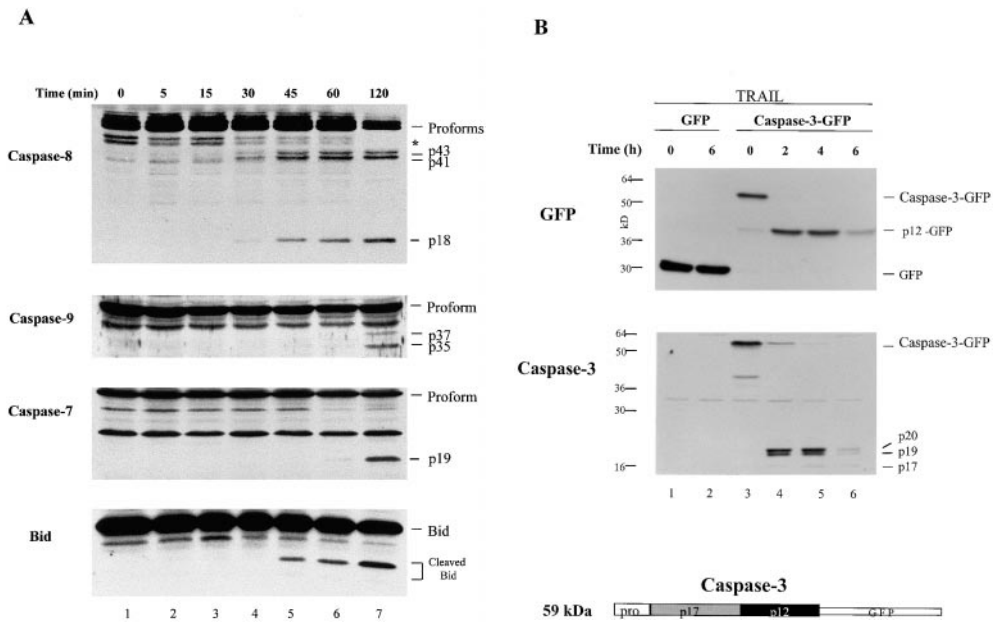

Figure 1. Caspase-8 is the most apical caspase in TRAIL-induced apoptosis in MCF-7 cells. (A) MCF-7 cells were incubated for up to 2 h, either alone or in the presence of recombinant TRAIL (1 μg/ml) and the time course of cleavage of the initiator caspases-8 and -9, the effector caspase-7, and the regulatory molecule Bid were assessed by Western blot analysis as described in Materials and Methods. The asterisk marks nonspecific protein bands detected by the caspase-8 antibody in MCF-7 cells. (B) MCF-7 cells were transiently transfected with pEGFP-N1 or caspase-3-GFP and, 16 h after transfection, were incubated for up to 6 h with recombinant TRAIL (1 μg/ml). Cells were analyzed by immunoblotting using an anti-GFP antibody (top) or an antibody that recognizes the p17 subunit of caspase-3 (bottom). The caspase-3-GFP structure outlines the boundaries of the two caspase subunits and the NH_2-terminal prodomain (Pro). Cleavage to generate fully processed enzyme occurs at Asp-175, Asp-9, and Asp-28.

chrome *c*. Therefore, we wished to investigate whether cleavage of Bid also occurred during TRAIL-induced apoptosis. Bid was present in MCF-7 cells as a 26-kD protein, which, after exposure to TRAIL, was cleaved initially to yield a major fragment of 15 kD together with a minor 13-kD fragment. This cleavage was first observed at 45 min (Fig. 1 A), which is consistent with an early activation of caspase-8. Our data demonstrate the sequential activation of caspase-8 and Bid, followed by activation of caspases-7 and -9. These results support the hypothesis that caspase-8 is the apical caspase in TRAIL-induced apoptosis.

Redistribution of Caspases-3, -7, and -8 during TRAIL-induced Apoptosis in MCF-7 Cells

We have previously shown that a redistribution of effector caspases occurs during CD95-induced apoptosis in vivo (Chandler et al., 1998). Therefore, we wished to investigate the subcellular distribution of caspases in intact cells during TRAIL-induced apoptosis. As our polyclonal antibodies to caspases-7 and -8 were unsuitable for immunocytochemistry, we constructed initiator and effector caspases containing green fluorescent protein (GFP) at their COOH termini (Fig. 1 B). To facilitate the localization of these GFP-tagged caspases, they were transiently transfected into MCF-7 cells, an adherent cell line. To ensure that GFP fusion at the COOH terminus did not affect the activation of caspases, caspase-3-GFP–transfected cells were analyzed by immunoblotting (Fig. 1 B). As MCF-7 cells contain no endogenous caspase-3 (Jänicke et al., 1998), analysis of caspase-3-GFP activation during TRAIL-induced apoptosis was possible using antibodies specific to either GFP or caspase-3. In cells transfected with GFP alone, no significant decrease in GFP protein levels was observed after treatment with TRAIL for 6 h (Fig. 1 B, top, lanes 1 and 2). Transfection of caspase-3/GFP, and subsequent exposure to TRAIL, resulted in a time-dependent processing of caspase-3-GFP to yield a fragment of 37 kD (Fig. 1 B, top, lanes 3–6). This cleavage product represents the p12 subunit of caspase-3 fused to GFP, and is the product of cleavage at Asp-175. Western blot analysis using a caspase-3–specific antibody confirmed that the MCF-7 cells used in this study were caspase-3 null (Fig. 1 B, bottom, lanes 1 and 2), and that TRAIL-induced apoptosis of cells transfected with caspase-3-GFP was associated with time-dependent processing of intact caspase-3-GFP to fragments of p20, p19, and p17 (Fig. 1 B, bottom, lanes 3–6). In addition, lysates prepared from cells transfected with caspase-3-GFP exhibited an increased (3.9 nmol/mg/min) caspase-3–like DEVDase activity when compared with lysates obtained from control MCF-7 cells (0.2 nmol/mg/min). Thus, GFP fusion at the COOH terminus of caspase-3 did not interfere with the TRAIL-induced processing of this molecule at Asp-9, Asp-28, or Asp-175 (Fernandes-Alnemri et al., 1996). Similarly, GFP fusion at the COOH terminus of caspase-7 did not affect its activation (data not shown).

Confocal analysis of control MCF-7 cells transfected with GFP-tagged caspases-3, -7, or -8, demonstrated a similar pattern of diffuse cytoplasmic staining for all three caspases (Fig. 2, C, E, and G). Counterstaining of the nuclei in control cells, with propidium iodide, confirmed that the subcellular distribution of caspases-3, -7, and -8 in these cells was primarily cytosolic (Fig. 2, C, E, and G). After treatment with TRAIL for 6 h, MCF-7 cells displayed several characteristic features of adherent cells undergoing apoptosis including cell shrinkage and nuclear condensation (Fig. 2, B, D, F, and H). In MCF-7 cells transfected with GFP-tagged caspases-3 and -7, a dramatic

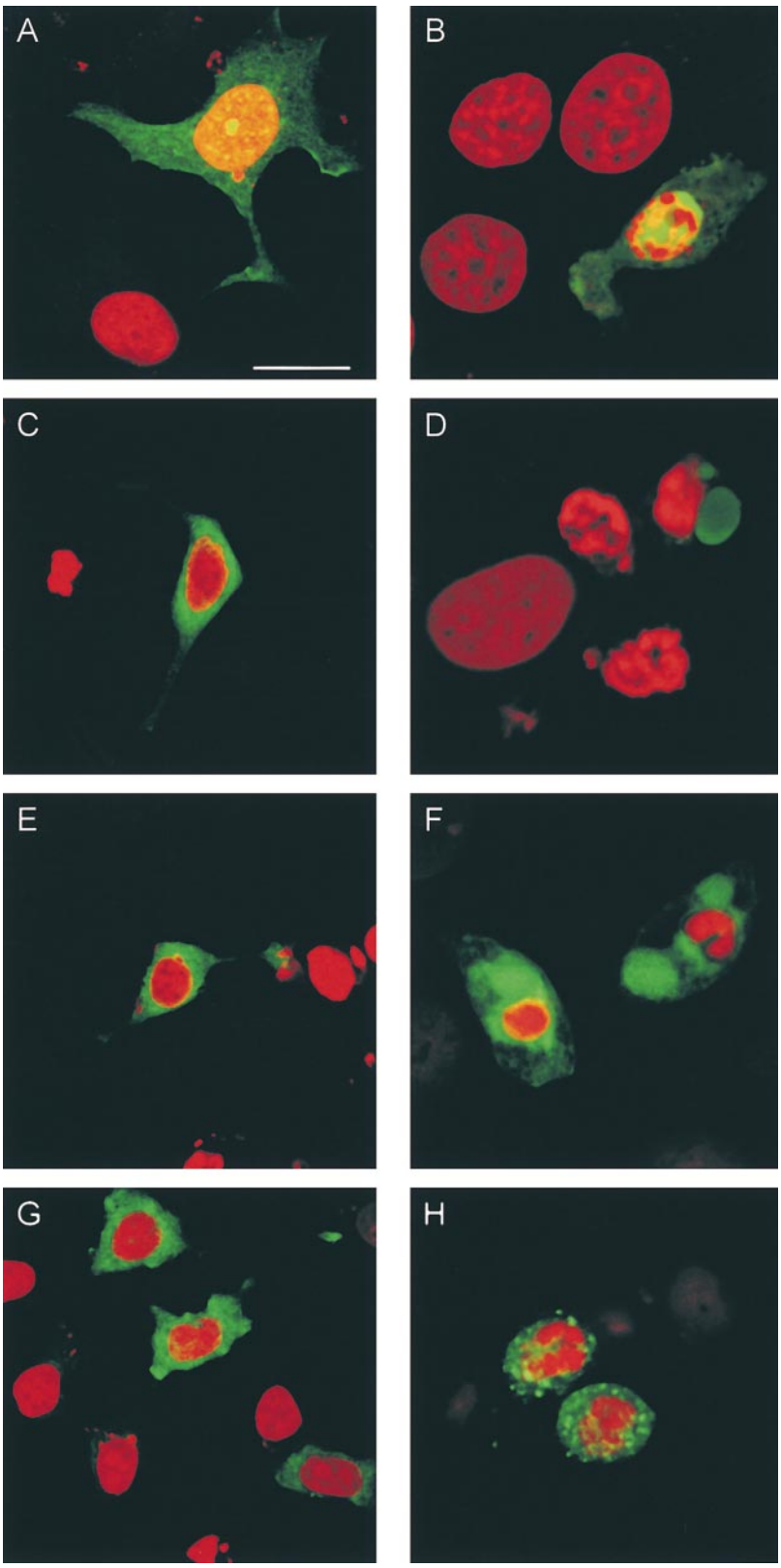

Figure 2. TRAIL-induced apoptosis results in redistribution of caspases-3, -7, and -8. MCF-7 cells were transiently transfected with pEGFP-N1 (A and B), caspase-3-GFP (C and D), caspase-7-GFP (E and F), or caspase-8–GFP (G and H). At 24 h after transfection, cells were incubated either alone (A, C, E, and G) or in the presence of recombinant TRAIL (1 μg/ml; B, D, F, and H) for 6 h, stained with propidium iodide to label DNA, and analyzed by confocal microscopy. GFP exhibits an even cellular distribution: orange/yellow fluorescence being evident in the nucleus because of colocalization of GFP and propidium iodide. Note the redistribution of caspases-3 and -7-GFP into large spheroidal inclusions in apoptotic MCF-7 cells, whereas caspase-8 exhibits a discrete punctate distribution in cells exhibiting altered nuclear morphology. Bar, 10 μm.

redistribution of green fluorescence into large spheroidal inclusions was clearly visible in the cytoplasm of apoptotic cells (Fig. 2, D and F). Interestingly, in these cells, almost all of the active effector caspases were redistributed into the large inclusions, with little active caspase detectable elsewhere in the cell (Fig. 2, D and F). In contrast, treatment of cells with TRAIL resulted in a redistribution of active caspase-8 into small punctate inclusions in the cytoplasm of apoptotic cells (Fig. 2 H). Treatment of MCF-7 cells with anti-CD95 resulted in similar changes in caspase

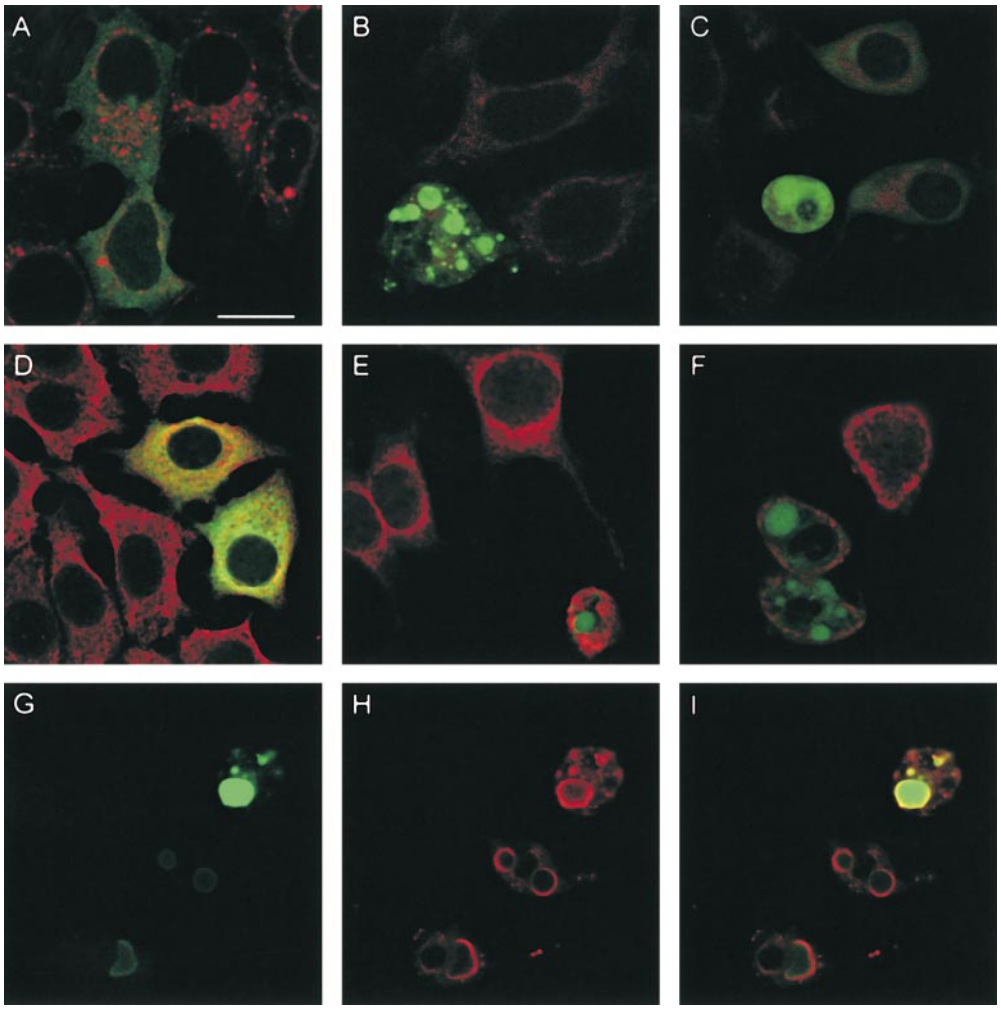

Figure 3. TRAIL-induced apoptosis results in colocalization of active transfected effector caspases and cleaved cytokeratin 18 in MCF-7 cells. MCF-7 cells were transiently transfected with caspase-3-GFP (A, B, D, and E) or caspase-7-GFP (C and F) and, 24 h later, the cells were treated with recombinant TRAIL (1 μg/ml; B, C, E and F) for 6 h. Cells were stained either with MitoTracker red (A–C) or by indirect immunofluorescence for calnexin (D–F). (G–I) MCF-7 cells were transfected with caspase-3-GFP and, 16 h later, were treated with recombinant TRAIL (1 μg/ml) for 6 h. (G) Confocal analysis demonstrates the redistribution of caspase-3-GFP into large spheroidal inclusions in apoptotic cells. (H) Indirect immunofluorescence with antibody M30, which recognizes a neo-epitope in K18 at DALD^{397}↓S, confirmed that the caspase-3-GFP–containing spheroidal inclusions also contained cleaved cytokeratin 18. I is an overlay of images G and H, demonstrating the colocalization of caspase-3-GFP and cleaved cytokeratin 18 in apoptotic cells. Bar, 10 μm.

distribution (data not shown). Thus, after TRAIL or CD95-induced apoptosis, a marked redistribution of caspases was observed, which differed between the effector caspases-3 and -7 and the initiator caspase-8.

Neither Mitotracker nor Calnexin Colocalize with GFP-tagged Caspases-3, -7, or -8

The TRAIL-induced redistribution of GFP-tagged caspases-3, -7, and -8 into intracytoplasmic spheroidal inclusions led us to investigate the nature of these structures. Using the selective dye MitoTracker red, mitochondria were clearly visible by confocal microscopy in control MCF-7 cells as discrete punctate structures throughout the cytoplasm, particularly in the perinuclear region (Fig. 3 A). No colocalization of caspase-3 with the mitochondria of MCF-7 cells was apparent when this distribution was compared with that of the GFP-tagged caspase-3. Treatment of caspase-3–transfected cells with TRAIL, followed by costaining with MitoTracker red, confirmed the subcellular redistribution of GFP-tagged caspase-3 into large spheroidal inclusions, and revealed that these structures were distinct from the mitochondria of apoptotic cells (Fig. 3 B). Similarly, no colocalization of calnexin, an ER transmembrane protein, was observed with either GFP-tagged caspase-3 in control MCF-7 cells (Fig. 3 D) or with the caspase-associated spheroidal inclusions induced by TRAIL (Fig. 3 E). Induction of apoptosis by TRAIL in caspase-7–transfected MCF-7 cells again resulted in the formation of large spheroidal inclusions that did not colocalize with mitochondria or the ER (Fig. 3, C and F). Similarly, actin, a major component of the cytoskeleton, did not colocalize with caspase-3 or -7 in control MCF-7 cells or after TRAIL treatment (data not shown). Furthermore, the small punctate inclusions detected in TRAIL-induced apoptotic MCF-7 cells transfected with GFP-tagged caspase-8 did not colocalize with mitochondria, ER, or the actin cytoskeleton (data not shown).

TRAIL Induces Spheroidal Inclusions in the Cytoplasm of Untransfected and Transfected MCF-7 Cells

The identity of the GFP-tagged caspase-3 and caspase-7–associated spheroidal inclusions in TRAIL-treated MCF-7 cells was further examined at the ultrastructural level. Initially, we confirmed that these inclusions were also formed in untransfected cells. Sections through untreated cultures showed a predominance of large cells, up

Table I. TRAIL Induces Cytokeratin-containing Inclusions in Epithelial Cells

	Percentage of cells containing inclusions				
	Control	TRAIL			
Cell line	Adherent cells	Adherent cells		Nonadherent cells	
MCF-7	0	4	(0.7)*	12	(0.8)
A549	0	6	(1.5)	93	(6.0)
HBL100	0	<1	(0.5)	64	(0.8)

Cells were treated with TRAIL (1 μg/ml) for 7 h and nonadherent cells were centrifuged. Insufficient nonadherent cells were obtained in control cultures to yield a cell pellet. Both adherent and nonadherent cells were fixed and labelled with immunogold using a mixture of mAbs to cytokeratins 8, 18, and 19. The percentage of cells containing cytokeratin inclusions was determined. Intermediate filaments were positively labelled in all untreated cells.

*The number in parentheses indicates the maximum diameter (expressed in μm) of the cytokeratin-containing inclusions.

to 15 μm in diameter, which were interconnected by tight junctions (Fig. 4 A). The electron lucent cytoplasm contained a diffuse network of microfilaments and intermediate filaments. The nuclear profiles were regular and characterized by a thin rim of heterochromatin lining the inner membrane of the nuclear envelope. Treatment of untransfected MCF-7 cells with TRAIL (Fig. 4, B and C) or anti-CD95 (data not shown) resulted in the formation of apoptotic cells with a cytoplasm, which was particularly electron dense even in the absence of fixation with osmium tetroxide. The apoptotic MCF-7 cells were also characterized by nuclei with clumps of moderately condensed perinuclear chromatin that extended into the nucleoplasm, ultracondensed mitochondria, dilation of the ER, and distinct sheaves of filaments (Fig. 4 B). In some apoptotic cells, small cytoplasmic inclusions (<1 μm diam) of a fine amorphous material were also observed (Table I). These inclusions (Fig. 4, B and C) were sharply demarcated from the surrounding cytoplasm but, like the actin-rich structures reported in the cytoplasm of apoptotic monocytes (Dinsdale et al., 1999), they were devoid of any limiting membrane. The nuclear changes observed contrast with the classical apoptotic characteristic of sharply delineated dense chromatin crescents abutting the inner nuclear membrane. This intermediate stage of chromatin condensation observed in apoptotic MCF-7 cells, is almost certainly the result of these cells being caspase-3 null (F. Li et al., 1997; Jänicke et al., 1998).

Ultrastructural analysis of MCF-7 cells transfected with either Lipofectamine or GFP alone revealed the majority of these cells to be indistinguishable from control cells (data not shown). Treatment of untransfected cells with TRAIL for 7 h, resulted in the induction of apoptosis and the presence of keratin-containing inclusions in 12% of nonadherent cells (Table I). When cells transfected with GFP-tagged caspases-3 or -7 were exposed to TRAIL, there was a marked increase in apoptotic cells with a striking presence of many more and larger cytoplasmic inclusions (Fig. 4 D) associated with loss of cytoplasmic filaments. These larger inclusions were spheroidal, up to 5 μm in diameter, and apparently formed by fusion of numerous smaller inclusions (data not shown). Transfected cells with large inclusions showed more pronounced nuclear changes than cells treated with TRAIL alone. These nuclear changes usually included disruption or loss of the nuclear envelope and dispersal of the nucleolus (Fig. 4 D). Similar nuclear changes and large cytoplasmic spheroidal inclusions were observed after anti-CD95 treatment of cells transfected with GFP-tagged caspase-3 or -7 (data not shown). In contrast, cells treated with TRAIL or anti-CD95 after transfection with caspase-8 did not undergo either of these changes. However, these cells contained the small cytoplasmic inclusions observed in nontransfected cells that had been treated with these agents (data not shown). Thus, transfection with GFP-tagged caspases-3 or -7, but not caspase-8, followed by treatment with TRAIL or anti-CD95 resulted in an exaggerated apoptotic phenotype compared with cells treated with TRAIL or anti-CD95 alone. This exaggerated phenotype was characterized by pronounced nuclear disruption and the formation of the large spheroidal inclusions (Fig. 4, compare B and D), which corresponded in size and distribution to those observed by confocal microscopy (Figs. 2 and 3).

Cytokeratins 8, 18, and 19 Are Redistributed into the Large Spheroidal Inclusions

TRAIL-induced formation of large spheroidal inclusions in cells transfected with effector caspases was accompanied by the loss of detectable cytofilaments (Fig. 4 D); therefore, the subcellular distribution of cytofilament proteins in apoptotic cells was investigated. Immunogold labeling of ultrathin sections indicated that the spheroidal inclusions contained cytokeratins but not β-actin, tubulin, or vimentin. A specific mAb to K18 produced intense, specific immunogold labeling of the spheroidal inclusions of cells transfected with GFP-tagged caspase-3 or -7 and treated with TRAIL (Fig. 5 A and data not shown). Intermediate filament disorganization and reorganization occurs during mitosis and is associated with phosphorylation, primarily on serine 53 of K18 (Ku and Omary, 1994). Immunogold labeling with antibody 3055, which specifically recognizes the K18 phosphorylated on serine 53 (P-K18; Liao et al., 1995), clearly demonstrated its accumulation in the spheroidal inclusions (Fig. 5 D). mAbs specific to the two other major cytokeratins present in MCF-7 cells, namely K8 and 19 (Moll et al., 1982), also labeled these spheroidal inclusions, whereas antibodies to K13, 15, and 16 did not (data not shown). There were no obvious inclusions in untreated MCF-7 cells, but the filament network was labeled by K8, 18, and 19 (Fig. 5 B, inset, and data not shown). In nontransfected TRAIL-treated cells, these antibodies labeled the distinctive sheaves of filaments (Fig. 5 B) and the small inclusions, which characterized these cells. In contrast, antibody M30, which specifically recognizes a caspase cleavage site within K18, did not label either the filament network or the sheaves of filaments (data not shown), but it did label the spheroidal inclusions (Fig. 5 C). M30 recognizes a neo-epitope, $DALD^{397}$, in the COOH terminus of K18 exposed early during apoptosis (Leers et al., 1999). Furthermore, colabeling of the spheroidal inclusions with antibody 3055 (5 nm immunogold) and the M30 antibody (10 nm immunogold) was also observed (Fig. 5 D). Thus, the distinctive large spheroidal inclusions in apoptotic MCF-7 cells contained K8, 18, and 19 as well as P-K18, and resulted from redistribution and cleavage of the intermediate filaments.

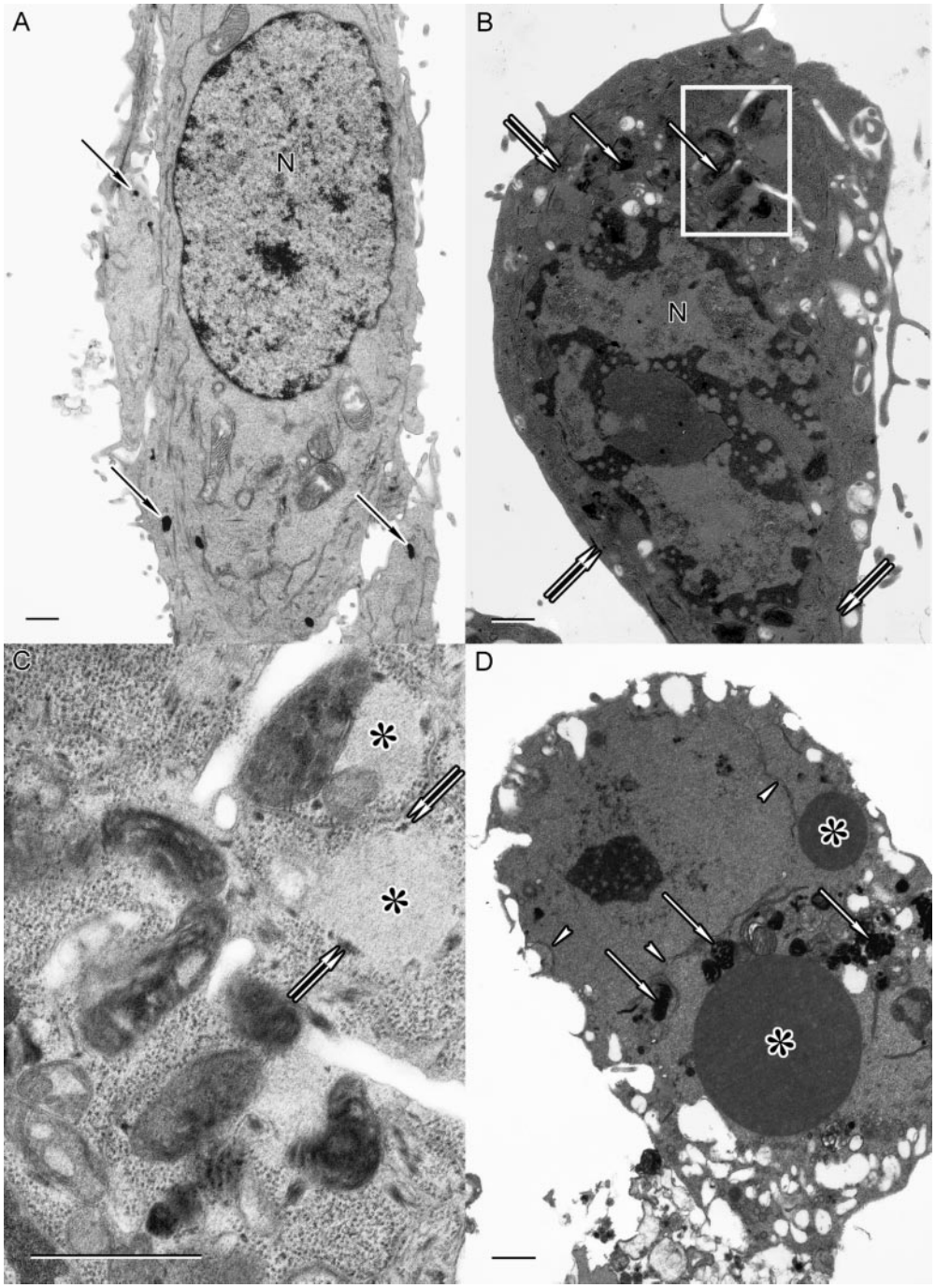

Figure 4. Ultrastructural changes in untransfected and caspase-3–transfected MCF-7 cells after treatment with TRAIL. (A) The electron lucent cytoplasm of an untreated cell contains a diffuse network of filaments. A few short microvilli are present on the apical membranes and small osmiophilic granules (black arrows) are evident in the underlying cytoplasm. The nucleus (N) is regular and characterized by a thin rim of heterochromatin. (B) An untransfected cell, 6 h after treatment with TRAIL, showing a scalloped nucleus (N) containing clumps of moderately condensed chromatin that extend to the nucleolus. The characteristic electron dense cytoplasm of this cell contains ultracondensed mitochondria (white arrows), distinct sheaves of filaments (double white arrows), and small inclusions of a fine amorphous material (outlined area). (C, detail from area outlined in B) The cytoplasmic inclusions (asterisk) are devoid of any limiting membrane, but some sheaves of filaments (double white arrows) are associated with their periphery. (D) A cell from a culture transfected with caspase-3, and treated with TRAIL for 6 h, showing disruption of the nuclear envelope (white arrowheads) and dispersal of the nucleolus. The cytoplasm contains numerous ultracondensed mitochondria (white arrows) and two large spheroidal inclusions (asterisk) that consist of a fine amorphous material. Bars, 1 μm.

TRAIL-induced Colocalization of Active Effector Caspases and Cleaved Cytokeratin 18

We wished to determine whether the GFP-containing spheroidal inclusions observed by confocal microscopy in TRAIL-induced MCF-7 cells transfected with GFP-tagged caspases-3 and -7 (Fig. 2, D and F) were associated with cleaved cytokeratins. Using the M30 antibody, we performed immunocytochemistry on caspase-3-GFP–transfected MCF-7 cells that had been exposed to TRAIL for 6 h. Immunolabeling for cleaved K18 was only present in apoptotic cells and was predominantly localized in discrete cytoplasmic structures and on the periphery of large spheroidal inclusions (Fig. 3 H), which resembled those inclusions previously shown to contain caspase-3 or -7 in transfected cells (Figs. 2, D and F, and 3 G). As antibody M30 only recognizes cleavage of K18 at $DALD^{397}\downarrow S$, we cannot exclude the possibility that cleavage at $VEVD^{238}\downarrow A$ has also occurred either before or in parallel with sequestration of cleaved K18 into spheroidal inclusions after TRAIL-induced apoptosis. Preferential immunolabeling

of the periphery of inclusions by antibody M30 was almost certainly the result of their impermeability to antibodies as immunogold studies, using ultrathin sections, showed uniform labeling throughout the inclusions (Fig. 5 D). Despite these difficulties with antibody accessibility, it was evident that GFP-tagged caspase-3 and cleaved K18 were colocalized in large spheroidal inclusions present in MCF-7 cells after exposure to TRAIL (Fig. 3 I). Similar results were obtained when HeLa cells, transfected with caspase-3- or -7-GFP and exposed to TRAIL, were colabeled with antibody M30 (data not shown). Thus, activated caspases-3 and -7 are associated with cleaved K18 in apoptotic MCF-7 cells, further supporting the hypothesis that effector caspases are primarily responsible for the ordered dismantling of the filament structure in epithelial cells during apoptosis.

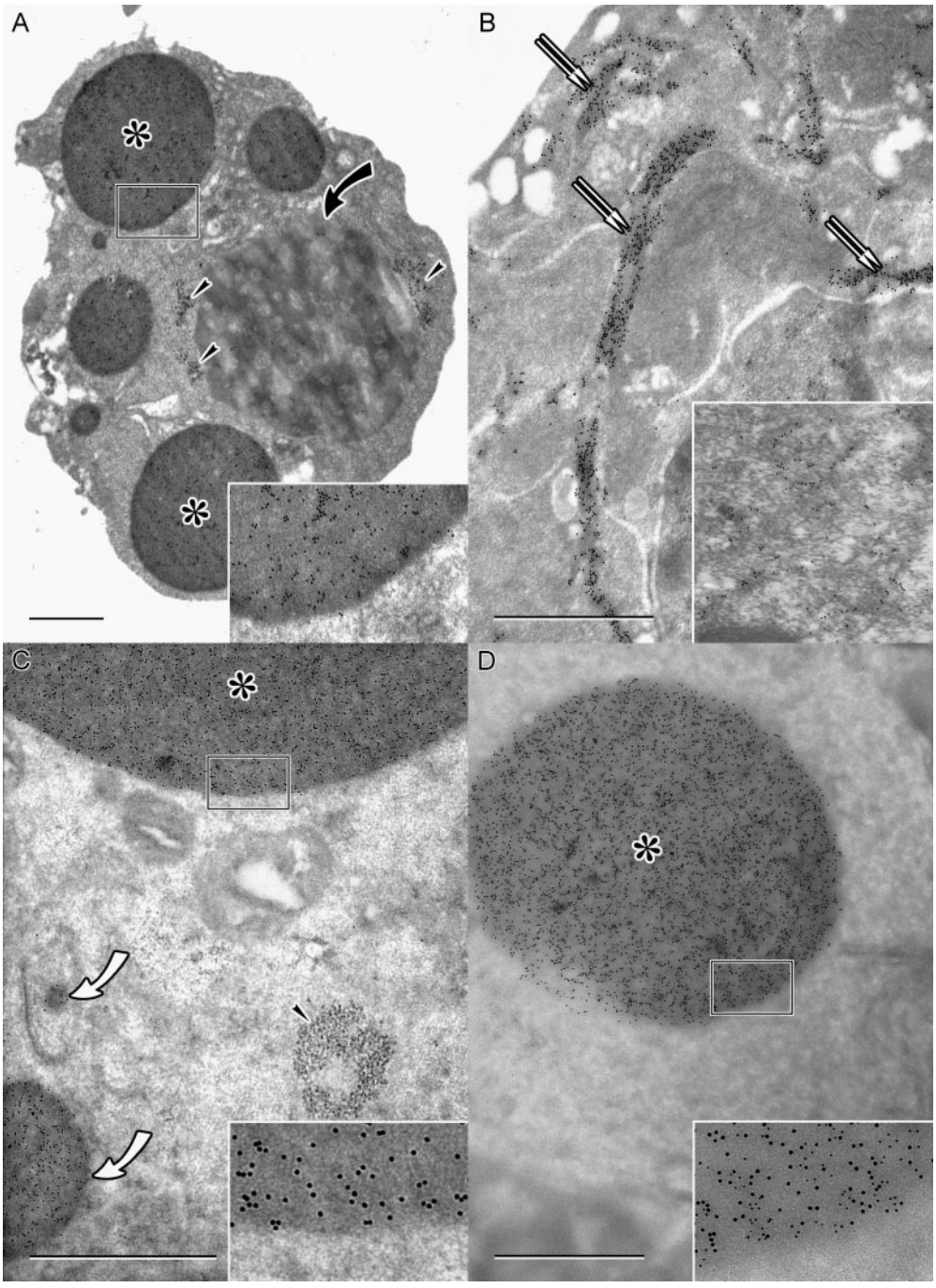

Figure 5. Ultrastructural localization of cytokeratins in control, caspase-3, and caspase-7–transfected MCF-7 cells after treatment with TRAIL. (A) The cytoplasm of a cell transfected with caspase-3, and exposed to TRAIL for 6 h, is largely devoid of labeling for K18, but the label is concentrated over large (asterisks) and small spheroidal inclusions. Remnants of the dense, fibrillar component (black arrowheads) are evident alongside the enlarged granular component (curved black arrow) of the nucleolus. The inset is a threefold magnification of the area outlined. (B) In a nontransfected cell, exposed to TRAIL for 6 h, K18 is localized in sheaves (double white arrows) present throughout the cytoplasm. The inset shows the diffuse distribution of cytokeratin 18–labeled intermediate filaments in control cells. (C) The cytoplasm of a cell transfected with caspase-7, and exposed to TRAIL for 6 h, contains a large spheroidal cytoplasmic inclusion (asterisk), together with two smaller inclusions (curved white arrows) which are labeled with 10 nm immunogold after incubation with the M30 antibody, which is specific to the cleaved form of K18. The rest of the cell, including a remnant of the nucleolar dense fibrillar component (black arrowhead) is devoid of label. The inset is a threefold magnification of the area outlined. (D) The cytoplasm of a cell transfected with caspase-7 and exposed to TRAIL for 6 h. Labeling by both the M30 antibody (10 nm immunogold) and the 3055 antibody, which is specific to the phosphorylated form of this cytokeratin (5 nm immunogold), is evident over a large spheroidal inclusion (asterisk). The inset is a threefold magnification of the area outlined. Bars, 1 μm.

Effector Caspases Induce Cleavage of Cytokeratins 8, 18, and 19 during TRAIL-induced Apoptosis

To determine the integrity and phosphorylation state of the cytokeratin proteins during apoptosis, MCF-7 cells were transfected with caspase-7-GFP, treated with TRAIL for 5 h, and sorted into two populations containing either untransfected cells or cells transfected with caspase-7-GFP (Fig. 6 A). Control MCF-7 cells contained K8, 18, and 19 as intact proteins of 52, 48, and 40 kD, respectively. Treatment of untransfected or caspase-7-GFP–transfected MCF-7 cells with TRAIL resulted in cleavage of K19 to yield a fragment of ~38 kD and cleavage of K8 to yield a fragment of ~46 kD and possibly one of ~48 kD (Fig. 6 A). Cleavage of both K8 and K19 has been reported during radiation-induced apoptosis of breast tumor cells (Prasad et al., 1998). Although K8 cleavage also occurs in the nonsmall-cell lung cancer cell line, MRC65 (van Engeland et al., 1997), its cleavage may be a cell type–specific phenomenon as it is relatively spared during apoptosis of several other epithelial cell types (Caulin et al., 1997; Ku et al., 1997). In the MCF-7 cells treated with TRAIL for 5 h, K18 was cleaved to yield a fragment of ~26 kD but, in the cells transfected with caspase-7-GFP, an additional cleavage product of ~19 kD was also detected (Fig. 6, A lane 3). This result implicated effector caspases in the degradation of the cytoskeleton in agreement with previous work that identified a specific caspase cleavage site in K18 during drug and UV-induced apoptosis (Caulin et al., 1997). Using recombinant caspases as well as various mutants, these authors demonstrated that caspase-3, -6, or -7 could cleave K18 at VEVD^{238}↓A, located within the non-α-helical L1-2 linker region, yielding a 26-kD NH_2-terminal and a 22-kD COOH-terminal fragment. A caspase-3 or -7 COOH-terminal cleavage site, which results in cleavage of intact K18 to a 45-kD fragment or further processing of the 22-kD fragment to an ~19-kD fragment, was also noted but not identified (Caulin et al., 1997).

To further investigate the role of caspases in TRAIL-induced cleavage of cytokeratins, we exposed either control or transfected MCF-7 cells to TRAIL in the presence of two caspase inhibitors (Fig. 6 B). z-VAD.FMK is a broad spectrum caspase inhibitor, whereas YVAD.CMK is reported to be more specific for caspases-1 and -6 (Lazebnik et al., 1995; MacFarlane et al., 1997b). Treatment of control MCF-7 cells, or cells transfected with GFP alone, with TRAIL for 7 h resulted in cleavage of K18 to yield four immunoreactive products of ~45, 26, 22, and 19 kD (Fig. 6 B, lanes 2 and 4). In cells transfected with caspase-3-GFP either alone or treated with TRAIL, cleavage of K18 predominantly yielded the 19-kD product with small amounts of the other fragments (Fig. 6 B, lanes 5 and 6). The 26-kD but not the 22- or 19-kD fragments was also detected by the P-K18–specific antibody, 3055 (Fig. 6 B), supporting the suggestion that the 26- and 22-kD products are the NH_2 and COOH terminally derived fragments, respectively, resulting from cleavage at VEVD^{238}↓A (Fig. 6 C). The M30 antibody, which recognizes the neo-epitope DALD↓S, labeled the 19-kD but not the 26- or 22-kD fragments (data not shown), suggesting that the 19-kD product was derived from further cleavage of the ~22-kD product at DALD^{397}↓S (Fig. 6 C). Thus, in the absence

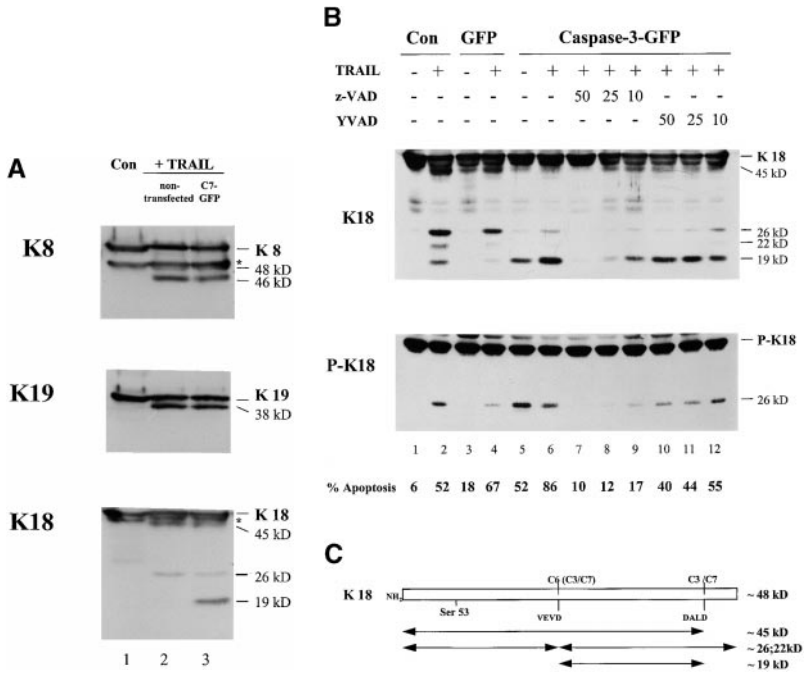

Figure 6. Cytokeratins 8, 18, and 19 together with P-K18 are cleaved by effector caspases during TRAIL-induced apoptosis. (A) MCF-7 cells were transiently transfected with caspase-7-GFP and, 24 h later, were incubated with recombinant TRAIL (1 μg/ml) for a further 5 h. Cells were sorted by flow cytometry into two populations of cells exposed to TRAIL: untransfected cells and those expressing caspase-7-GFP. Control cells contained primarily the intact forms of all three cytokeratins (lane 1). In cells treated with TRAIL, processing of K8, 18, and 19 was detected, with K18 being more extensively processed in cells expressing caspase-7-GFP (lanes 2 and 3, respectively). The asterisks mark nonspecific bands of ~49 and 47 kD detected by the K8 and K18 antibodies, respectively. (B) z-VAD.FMK blocks the cleavage of cytokeratins. MCF-7 cells were transiently transfected with pEGFP-N1 or caspase-3-GFP either in the absence or presence of YVAD.CMK (10–50 μM) or z-VAD.FMK (10–50 μM). Control cells, or cells transfected with GFP alone or caspase-3-GFP, were treated with recombinant TRAIL (1 μg/ml) for 7 h and analyzed by Western blot analysis. Extensive cleavage of K18 and P-K18, induced by transfection of caspase-3-GFP and a 7-h exposure to TRAIL, was blocked by z-VAD.FMK but only partially inhibited by YVAD.CMK. (C) A schematic representation of the potential fragments resulting from cleavage of K18 by effector caspases. The K18 antibody, CY90, detects intact K18 together with fragments of 45, 26, 22, and 19 kD. In contrast, antibody 3055, which is specific for K18 phosphorylated on serine 53, detects only K18 and a 26-kD fragment generated by cleavage at VEVD^{238}↓S.

of caspase-3, K18 was preferentially cleaved to a 26-kD fragment (Fig. 6 B, lanes 2 and 4), but in the presence of either caspase-3 (Fig. 6 B, lane 6) or caspase-7 (Fig. 6 A, lane 3), the additional 19-kD product was also observed. Pretreatment of cells with z-VAD.FMK (10–50 μM) inhibited apoptosis and cleavage of both K18 and P-K18 in a concentration-dependent manner (Fig. 6 B, lanes 7–9). Almost complete inhibition was observed at the highest concentration (Fig. 6 B, lanes 7–9), which is consistent with the ability of z-VAD.FMK to inhibit the proteolytic activity of all known caspases (Garcia-Calvo et al., 1998). YVAD.CMK (10–50 μM), which caused only a slight inhibition of apoptosis (Fig. 6 B), did not markedly inhibit the processing of K18 or P-K18 (Fig. 6 B, lanes 10–12). In contrast, in untransfected MCF-7 cells exposed to TRAIL, YVAD.CMK (25 μM) completely inhibited formation of the 26- and 19-kD cleavage products of K18 (data not shown), which is consistent with previous reports that cleavage of K18 at VEVD↓A, is primarily mediated by caspase-6. Thus, the inability of YVAD.CMK to significantly inhibit K18 cleavage in the presence of exogenously transfected caspase-3 or -7 (Fig. 6 B) is consistent with cleavage of K18 occurring, in this instance, at both the caspase-3 and/or -7 preferred site, DALD↓S and the VEVD↓A site normally preferred by caspase-6 (Fig. 6 C).

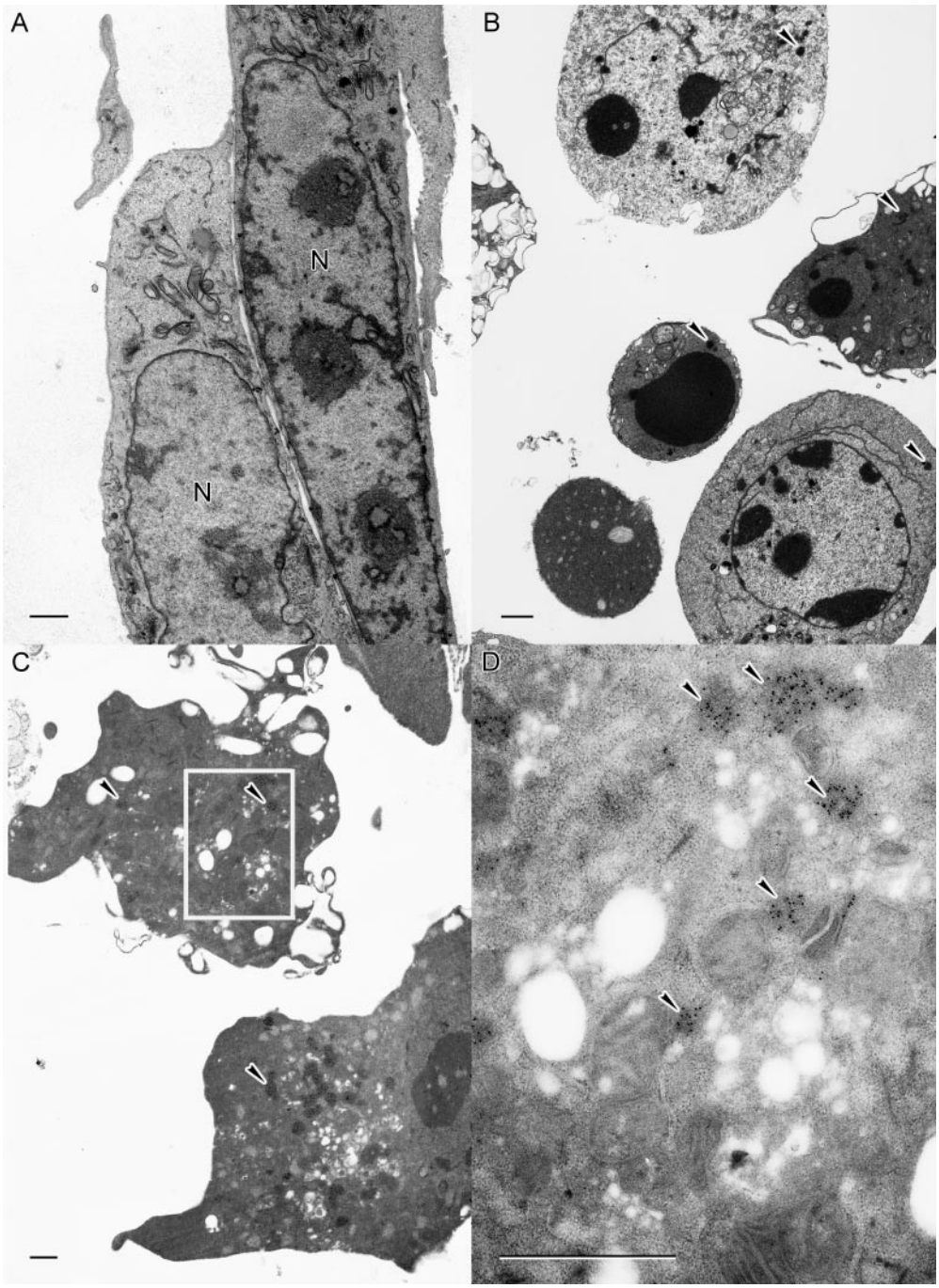

Figure 7. TRAIL induces spheroidal inclusions in HBL100 cells. (A) Untreated adherent HBL100 cells display a regular nucleus (N) and are devoid of cytoplasmic inclusions. (B) After exposure to TRAIL for 7 h, detached cells show characteristic apoptotic nuclear morphology and small spheroidal cytoplasmic inclusions (black arrowheads). (C and D) These inclusions (black arrowheads) contain cleaved K18 as shown by immunogold labeling with antibody M30. The inset in C is shown at a higher magnification in D. Bars, 1 μm.

Redistribution of Cleaved Cytokeratins into Spheroidal Inclusions Is a Characteristic Feature of Epithelial Cells Undergoing Apoptosis

We wished to determine whether the spheroidal inclusions observed in transfected or untransfected MCF-7 cells exposed to TRAIL (Figs. 4 and 5) were also evident in other epithelial cells undergoing apoptosis. HBL100, breast epithelial cells, and A549, type II lung cells, were exposed to TRAIL and examined by ultrastructural immunocytochemistry. Sections through untreated cultures of HBL100 (Fig. 7 A) and A549 (Fig. 8 A) cells showed a predominance of large adherent cells with regular nuclear profiles. Treatment of these cells with TRAIL resulted in an increased incidence of apoptotic cells, characterized by detachment, rounding-up and chromatin margination (Figs. 7 B and 8 B). The hypercondensed mitochondria observed in apoptotic MCF-7 cells (Fig. 4) and apoptotic THP.1 cells (Dinsdale et al., 1999) were not observed in either HBL100 or A549 cells, suggesting that these changes are only associated with the apoptotic phenotype of certain cells.

Apoptotic HBL100 cells were also characterized by the presence of small cytoplasmic inclusions (<1 μm diam) with an indistinct outline. These inclusions were labeled by antibodies to both intact (Table I) and cleaved K18 (Fig. 7,

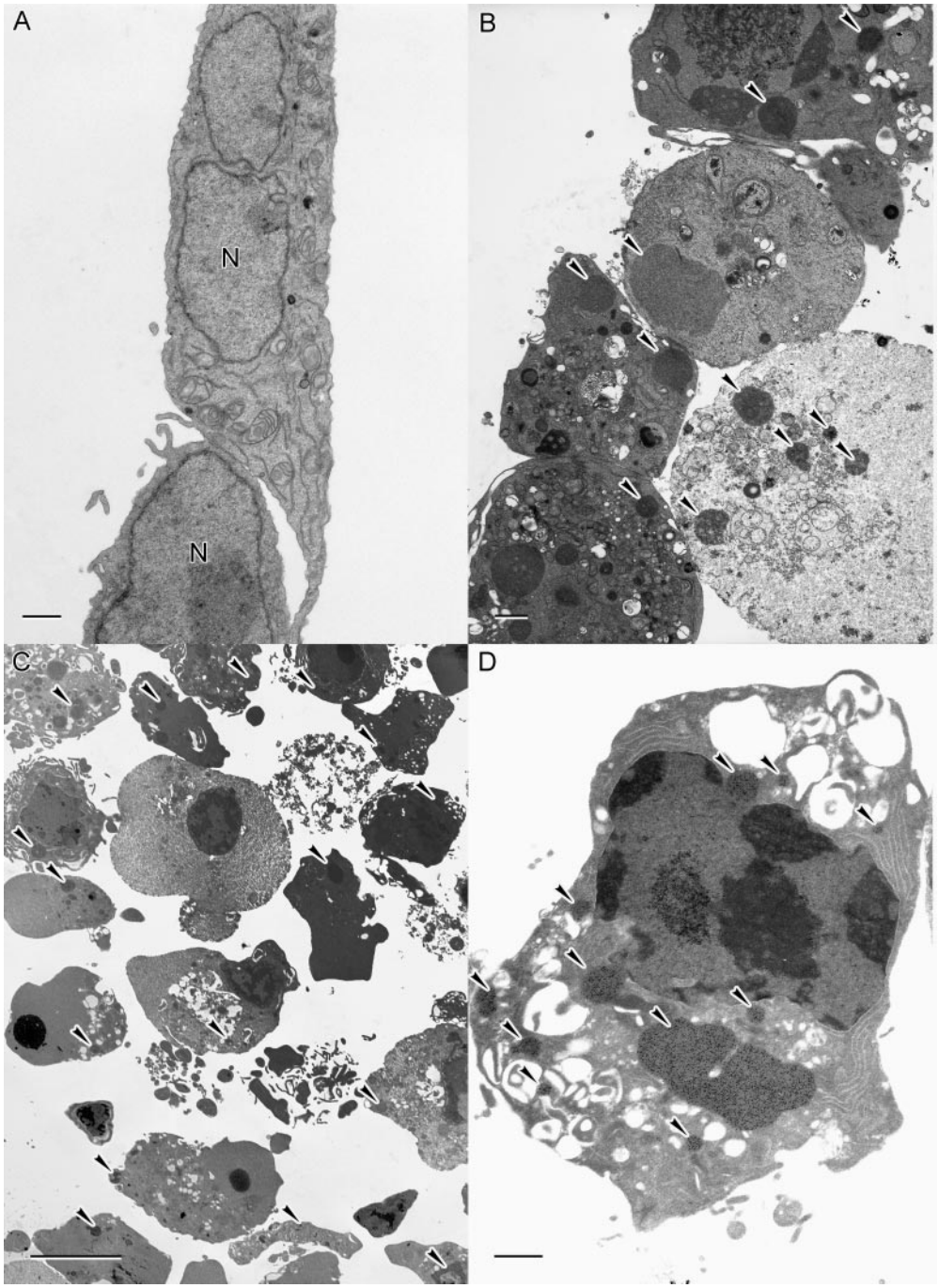

Figure 8. TRAIL induces spheroidal inclusions in A549 cells. (A) Untreated adherent A549 cells display a regular nucleus (N) and are devoid of cytoplasmic inclusions. (B) After exposure to TRAIL for 3 h, many detached cells display a characteristic apoptotic nuclear morphology and contain a range of spheroidal cytoplasmic inclusions (black arrowheads). (C) These inclusions contain K18 as shown by immunogold labeling. For clarity, only one inclusion/cell is marked (black arrowheads). (D) These inclusions (black arrowheads) also contain cleaved K18 as shown by immunogold labeling with antibody M30. Bars: (A, B, and D) 1 μm; (C) 10 μm.

C and D). In A549 cells exposed to TRAIL, many more and larger cytoplasmic inclusions were observed, and these were also labeled by both antibodies (Table I and Fig. 8, C and D). Thus, redistribution and cleavage of the cytokeratin network into cytoplasmic inclusions is a characteristic feature of a number of epithelial cell types undergoing apoptosis.

Trail-induced Colocalization of Active Endogenous Caspase-3 with Cleaved Cytokeratin 18 in Apoptotic Epithelial Cells

The recently characterized M30 antibody recognizes cleaved K18 in apoptotic cells, but does not recognize uncleaved K18 in viable or necrotic cells (Leers et al., 1999). In both untransfected MCF-7 and HBL100 cells exposed to TRAIL, M30 immunoreactivity was present only in apoptotic cells and localized in discrete cytoplasmic inclusions (Fig. 9, A and B). Similarly, the CM1 antibody recognizes only the p18 subunit but not the zymogen precursor of caspase-3 (Srinivasan et al., 1998). CM1 immunoreactivity was observed only in TRAIL-induced apoptotic HBL100 cells but not in nonapoptotic cells (Fig. 9 C). These studies confirmed the use of both these antibodies for specifically labeling apoptotic cells. Interestingly, both M30 (Fig. 9, A, B, D, and G) and CM1 (Fig. 9, C, E, and H) immunolabeling exhibited a discrete punctate cytoplasmic distribution in apoptotic cells. Furthermore, when apoptotic cells were colabeled with CM1 and M30 antibodies, the majority of active caspase-3 colocalized with the cytokeratin-containing inclusions (Fig. 9, D–I). These results demonstrated the redistribution and colocalization of both cleaved K18 and active endogenous caspase-3 into small cytoplasmic inclusions in both HBL100 and A549 cells undergoing apoptosis.

Discussion

TRAIL Initiates a Caspase Cascade with Caspase-8 at the Apex

Our demonstration of an early cleavage of caspase-8 and Bid, before activation of caspases-3 and -7, in MCF-7 cells (Fig. 1), strongly supports the hypothesis that caspase-8 is the most apical caspase in TRAIL-induced apoptosis. Activation of caspases-8 and -3 also has been observed in melanoma cells exposed to TRAIL (Griffith et al., 1998). Activated caspase-8 may either directly activate effector caspases or, via cleavage of Bid lead to the involvement of mitochondria, indirect activation of caspase-9, and downstream effector caspases. Cleavage of Bid, a caspase-8 substrate, only previously has been reported in CD95 and TNF-α–induced apoptosis (Li et al., 1998). However, our data

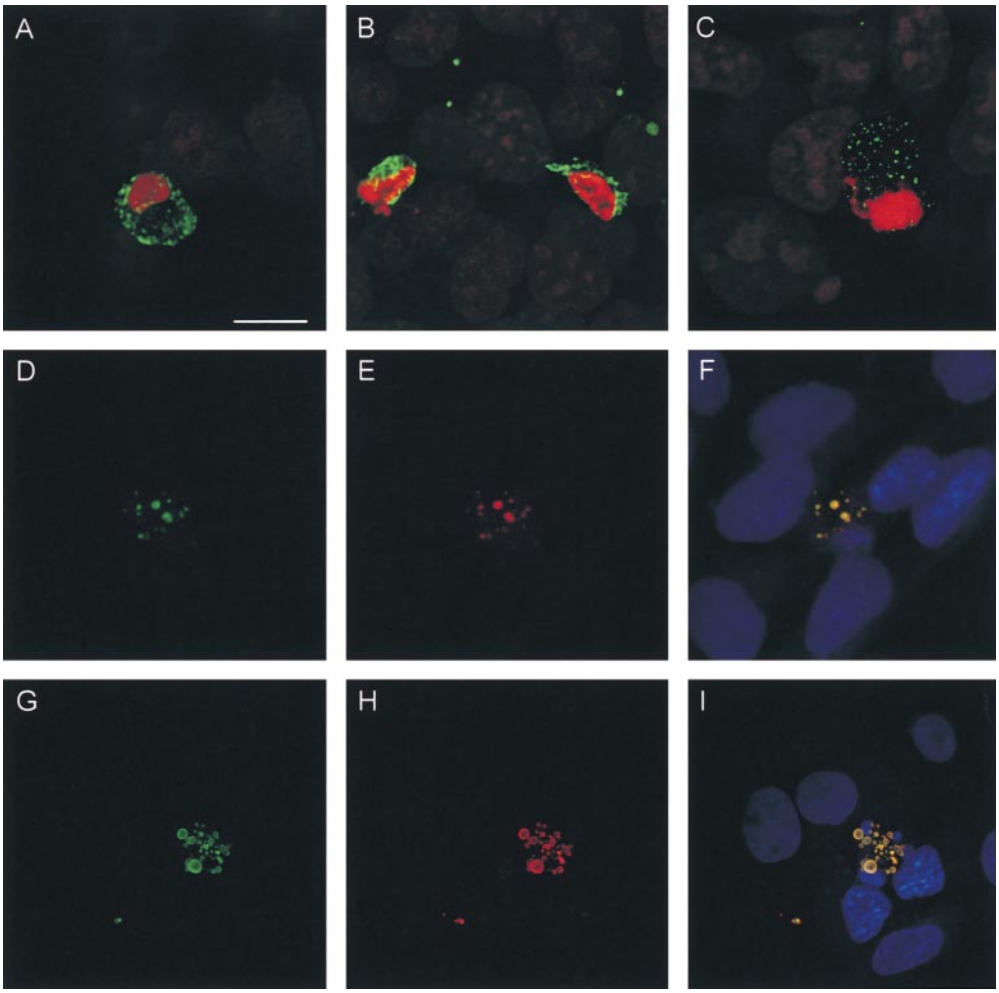

Figure 9. Active endogenous caspase-3 colocalizes with cleaved cytokeratin 18 in apoptotic epithelial cells. MCF-7 (A), HBL100 (B–F), and A549 (G–I) cells were treated with recombinant TRAIL (1 μg/ml) for 5 h, labeled with the appropriate antibody, and stained with propidium iodide (A–C) or Hoechst 33258 (F and I) to label DNA. Indirect immunofluorescence with antibody M30, confirmed the TRAIL-induced formation of spheroidal inclusions containing cleaved K18 specifically in apoptotic MCF-7 (A), HBL100 (B and D), and A549 cells (G). Indirect immunofluorescence, with antibody CM1, demonstrated that active caspase-3 was distributed in spheroidal inclusions specifically in apoptotic HBL100 (C and E) and A549 (H) cells. F is an overlay of images D and E, and I is an overlay of images G and H, demonstrating that the majority of active caspase-3 colocalizes with cleaved K18 in apoptotic HBL100 and A549 cells, respectively. Bar, 10 μm.

now demonstrate the participation of Bid in TRAIL-induced apoptosis. Recent studies using Bid-deficient mice have confirmed that Bid is a critical substrate for in vivo signaling by death receptor agonists, thereby mediating a mitochondrial amplification loop that is essential for apoptosis in selected cells (Yin et al., 1999).

After TRAIL-induced apoptosis, the initiator caspase-8 redistributed within the cytosol into discrete punctate structures (Fig. 2), whereas the effector caspases-3 and -7 redistributed into large spheroidal inclusions (Figs. 2 and 3). These differences between initiator and effector caspases further emphasize their fundamentally different roles in receptor-mediated apoptosis in epithelial cells. In mouse liver, caspases-3 and -7 are initially cytosolic but, after CD95-induced apoptosis, show a differential subcellular redistribution (Chandler et al., 1998). The proform of caspase-3 also has been found primarily in the cytosol together with small amounts in the mitochondria of several cell types from rat and human tissues (Mancini et al., 1998; Samali et al., 1998; Zhivotovsky et al., 1999). However, in the present study, no colocalization of caspase-3-GFP with the mitochondria of MCF-7 cells was observed (Fig. 3), which is in agreement with the finding that the ratio of cytosolic to mitochondrial procaspase-3 varies between different tissues (Samali et al., 1998).

Effector Caspases Promote an Exaggerated Apoptotic Phenotype

MCF-7 cells are caspase-3 null (F. Li et al., 1997; Jänicke et al., 1998) and, therefore, provide a good model to dissect the apoptotic pathways for which caspase-3 activation is necessary. Apoptosis in most cell types is not solely dependent on caspase-3, as mice with a homozygous deletion in the *CASP*-3 gene only exhibit hyperplasia and significant abnormalities in the brain (Kuida et al., 1996; Woo et al., 1998). Based on studies using caspase-3–null cells, it has been proposed that caspase-3 activity is required for DNA fragmentation and membrane blebbing (Jänicke et al., 1998; Zheng et al., 1998), but is not essential for induction of apoptosis by either CD95 or TNF (F. Li et al., 1997). In the current study, the intermediate stage of chromatin condensation observed in MCF-7 cells exposed to TRAIL (Fig. 4) can be attributed to a partial fragmentation of DNA into kilobase pair fragments in the absence of DNA ladders (Brown et al., 1993). Overexpression of caspase-3 or -7, but not caspase-8, in cells exposed to TRAIL resulted in a more exaggerated apoptotic phenotype with larger cytokeratin-containing cytoplasmic inclusions and more pronounced nuclear changes (Figs. 4 and 5). These results are consistent with cleavage by effector, but not initiator, caspases of intracellular substrates, such as DFF (Liu et al., 1997) and cytokeratins, with appropriate motifs (e.g., DxxD). This further emphasizes the marked differences between initiator and effector caspases.

TRAIL Induces the Redistribution of Effector Caspases into Cytokeratin-associated Spheroidal Inclusions

Cytokeratins comprise the major intermediate filaments in the cytoplasm of epithelial cells and help to maintain cellular integrity. Disintegration of these filaments, resulting in the concentration of cytokeratins within cytoplasmic inclusions, has been reported in vivo in the Mallory bodies of injured hepatocytes and also in vitro in mitotic epithelial cells (Franke et al., 1982). Similar inclusions are observed in adenovirus-infected HeLa cells after cleavage of K18 by the viral L3 proteinase (Chen et al., 1993). The significance of cytokeratin reorganization during apoptosis only recently has been examined (van Engeland et al., 1997). The redistribution of cytokeratins into granular structures enriched for phosphorylated K18 has been reported in apoptotic cells (Caulin et al., 1997; Ku et al., 1997). Primarily based on studies with recombinant proteins, this redistribution has been proposed to be dependent on cleavage of type I keratins by effector caspases. Interestingly, phosphorylation of K18 at serine 53 does not render K18 a better substrate for effector caspases (Caulin et al., 1997; Ku et al., 1997).

Our biochemical and ultrastructural data provide new insight on the fate of cytokeratins during apoptosis. On exposure to TRAIL, the cytokeratin bundles characteristic of control cells (Fig. 5 B, inset) reorganized into filament sheaves found either free in the cytoplasm or associated with the periphery of small inclusions containing K8, -18, and -19 (Figs. 4, B and C, and 5 B). Cytokeratin disassembly was primarily mediated by effector caspases, as these inclusions were larger and more pronounced in MCF-7 cells in the presence of exogenously expressed caspases-3 or -7. Both the inclusions and the filament sheaves contained the phosphorylated form of K18, whereas coimmunogold labeling with the M30 antibody demonstrated the presence of cleaved K18 only in the spheroidal inclusions (Fig. 5). These data are compatible with initial phosphorylation of K18 and the formation of filament sheaves, followed by cleavage of K18 at $DALD^{397}\downarrow S$, which results in the transformation of these sheaves into inclusions. However, we cannot exclude the possibility that the filament sheaves may contain K18 cleaved at other sites, such as $VEVD^{238}\downarrow A$, which would not be recognized by the M30 antibody.

Cytokeratin-associated Spheroidal Inclusions Are a Characteristic Feature of Epithelial Cell Apoptosis

Particularly striking was the finding of spheroidal inclusions in TRAIL-treated epithelial cells. While initially observed in MCF-7 cells transfected with caspases-3 or -7, they were subsequently observed in a variety of untransfected TRAIL-treated epithelial cells from the breast (MCF-7 and HBL100), lung (A549), and cervix (HeLa; Figs. 4, 7, and 8, and data not shown). These inclusions contained cleaved K18, which, in both A549 and HBL100 cells, colocalized with active endogenous caspase-3 (Fig. 9). Interestingly, the inclusions were more prevalent in untransfected HBL100 and A549 than in MCF-7 cells most probably because the A549 and HBL100 cells possess sufficient caspase-3 to cleave cytokeratins and form cytoplasmic inclusions. The formation of such inclusions appears to be a general feature of TRAIL-induced apoptosis of epithelial cells.

These observations raise the question as to why such inclusions are formed and why active effector caspases are sequestered within them. Active caspases may be required to ensure the ordered dismantling of the intermediate fila-

ment network in epithelial cells undergoing apoptosis. Effector caspases cleave several other cytoskeletal proteins including nuclear lamins, fodrin, and actin together with the cytoskeletal regulators Gas2 and gelsolin (Thornberry and Lazebnik, 1998); thus, reflecting the requirement for disassembly of the cytoskeleton during the execution phase of apoptosis. Alternatively, the sequestration and subsequent degradation of active effector caspases may prevent their escape from the cell and, therefore, their ability to damage healthy neighboring cells. This latter suggestion is compatible with the observation that apoptosis in tissues is normally limited to individual scattered cells (Arends and Wyllie, 1991). Sequestration of active effector caspases may be an important component of the cell death program required to prevent the spread of cell damage before removal of the apoptotic cell by phagocytosis. We demonstrate that cytokeratin disassembly and the formation of caspase-associated spheroidal inclusions occurs after TRAIL-induced apoptosis of lung, cervical, and nontransformed breast epithelial cells. Therefore, we propose that this phenomenon may be a characteristic feature of epithelial cells undergoing apoptosis.

We thank the following for supplying us with valuable reagents: E. Alnemri for caspase-3, -7 and -8 cDNA templates; D. Green for caspase-9 antibody; M. Jattella for MCF-7-Fas cells; D. Nicholson for caspase-3 antibody; B. Omary for antibody 3055; A. Srinivasan for CM1 antibody; and X. Wang for Bid antibody. We are grateful to Judy McWilliam and Tim Smith for preparation of samples for electron microscopy.

Submitted: 1 June 1999
Revised: 4 February 2000
Accepted: 4 February 2000

References

Arends, M.J., and A.H. Wyllie. 1991. Apoptosis: mechanisms and roles in pathology. *Int. Rev. Exp. Path.* 32:223–254.

Ashkenazi, A., and V.M. Dixit. 1998. Death receptors: signalling and modulation. *Science* 281:1305–1308.

Boldin, M.P., T.M. Goncharov, Y.V. Goltsev, and D. Wallach. 1996. Involvement of MACH, a novel MORT1/FADD-interacting protease, in Fas/APO-1- and TNF receptor-induced cell death. *Cell.* 85:803–815.

Brown, D.G., X.-M. Sun, and G.M. Cohen. 1993. Dexamethasone-induced apoptosis involves cleavage of DNA to large fragments prior to internucleosomal fragmentation. *J. Biol. Chem.* 268:3037–3039.

Caulin, C., G.S. Salvesen, and R.G. Oshima. 1997. Caspase cleavage of keratin 18 and reorganization of intermediate filaments during epithelial cell apoptosis. *J. Cell Biol.* 138:1379–1394.

Chandler, J.M., G.M. Cohen, and M. MacFarlane. 1998. Different subcellular distribution of caspase-3 and caspase-7 following Fas-induced apoptosis in mouse liver *J. Biol. Chem.* 273:10815–10818.

Chen, P.H., D.A. Ornelles, and T. Shenk. 1993. The adenovirus L3 23-kilodalton proteinase cleaves the amino-terminal head domain from cytokeratin 18 and disrupts the cytokeratin network of HeLa cells. *J. Virol.* 67:3507–3514.

Cohen, G.M. 1997. Caspases: the executioners of apoptosis. *Biochem. J.* 326:1–16.

Dinsdale, D., J. Zhuang, and G.M. Cohen. 1999. Redistribution of cytochrome *c* precedes the caspase-dependent formation of ultracondensed mitochondria, with a reduced inner membrane potential, in apoptotic monocytes. *Am. J. Pathol.* 155:607–618.

Earnshaw, W.C. 1995. Nuclear changes in apoptosis. *Curr. Opin. Cell. Biol.* 7:337–343.

Fernandes-Alnemri, T., R.C. Armstrong, J. Krebs, S.M. Srinivasula, L. Wang, F. Bullrich, L.C. Fritz, J.A. Trapani, K.J. Tomaselli, G. Litwack, and E.S. Alnemri. 1996. *In vitro* activation of CPP32 and Mch3 by Mch4, a novel human apoptotic cysteine protease containing two FADD-like domains. *Proc. Natl. Acad. Sci. USA.* 93:7464–7469.

Franke, W.W., E. Schmid, and C. Grund. 1982. Intermediate filament proteins in nonfilamentous structures: transient disintegration and inclusion of subunit proteins in granular aggregates. *Cell.* 30:103–113.

Garcia-Calvo, M., E.P. Peterson, B. Leiting, R. Ruel, D.W. Nicholson, and N.A. Thornberry. 1998. Inhibition of human caspases by peptide-based and macromolecular inhibitors. *J. Biol. Chem.* 273:32608–32613.

Griffith, T.S., W.A. Chin, G.C. Jackson, D.H. Lynch, and M.Z. Kubin. 1998. Intracellular regulation of TRAIL-induced apoptosis in human melanoma cells. *J. Immunol.* 161:2833–2840.

Jänicke, R.U., M.L. Sprengart, M.R. Wati, and A.G. Porter. 1998. Caspase-3 is required for DNA fragmentation and morphological changes associated with apoptosis. *J. Biol. Chem.* 273:9357–9360.

Kayalar, C., T. Örd, M.P. Testa, L. Zhong, and D.E. Bredesen. 1996. Cleavage of actin by interleukin 1β-converting enzyme to reverse DNase I inhibition. *Proc. Natl. Acad. Sci. USA.* 93:2234–2238.

Ku, N.-O., and M.B. Omary. 1994. Identification of the major physiologic phosphorylation site of human keratin 18: potential kinases and a role in filament reorganization. *J. Cell Biol.* 127:161–171.

Ku, N.-O., J. Liao, and M.B. Omary. 1997. Apoptosis generates stable fragments of human type I keratins. *J. Biol. Chem.* 272:33197–33203.

Kuida, K., T.S. Zheng, S. Na, C. Kuan, D. Yang, H. Karasuyama, P. Rakic, and R.A. Flavell. 1996. Decreased apoptosis in the brain and premature lethality in CPP32-deficient mice. *Nature.* 384:368–372.

Kuwana, T., J.J. Smith, M. Muzio, V. Dixit, D.D. Newmeyer, and S. Kornbluth. 1998. Apoptosis induction by caspase-8 is amplified through the mitochondrial release of cytochrome *c. J. Biol. Chem.* 273:16589–16594.

Lazebnik, Y.A., S.H. Kaufmann, S. Desnoyers, G.G. Poirer, and W.C. Earnshaw. 1994. Cleavage of poly (ADP-ribose) polymerase by a proteinase with properties like ICE. *Nature.* 371:346–347.

Lazebnik, Y.A., A. Takahashi, R.D. Goldman, G.G. Poirier, S.H. Kaufmann, and W.C. Earnshaw. 1995. Studies of the lamin proteinase reveal multiple parallel biochemical pathways during apoptotic execution. *Proc. Natl. Acad. Sci. USA.* 92:9042–9046.

Leers, M.P.G., W. Kölgen, V. Björklund, T. Bergman, G. Tribbick, B. Persson, P. Björklund, F.C.S. Ramaekers, B. Björklund, M. Nap, H. Jörnvall, and B. Schutte. 1999. Immunocytochemical detection and mapping of a cytokeratin 18 neo-epitope exposed during early apoptosis. *J. Pathol.* 187:567–572.

Li, F., A. Srinivasan, Y. Wang, R.C. Armstrong, K.J. Tamaselli, and L.C. Fritz. 1997. Cell-specific induction of apoptosis by microinjection of cytochrome *c. J. Biol. Chem.* 272:30299–30305.

Li, H., H. Zhu, C. Xu, and J. Yuan. 1998. Cleavage of BID by caspase 8 mediates the mitochondrial damage in the Fas pathway of apoptosis. 1998. *Cell.* 94:491–501.

Li, P., D. Nijhawan, I. Budiharjo, S.M. Srinivasula, M. Ahmad, E.S. Alnemri, and X. Wang. 1997. Cytochrome c and dATP-dependent formation of Apaf-1/caspase-9 complex initiates an apoptotic protease cascade. *Cell.* 91:479–489.

Liao, J., L.A. Lowthert, N.-O. Ku, R. Fernandez, and M.B. Omary. 1995. Dynamics of human keratin 18 phosphorylation: polarized distribution of phosphorylated keratins in simple epithelial tissues. *J. Cell Biol.* 131:1291–1301.

Liu, X., H. Zou, C. Slaughter, and X. Wang. 1997. DFF, a heterodimeric protein that functions downstream of caspase-3 to trigger DNA fragmentation during apoptosis. *Cell.* 89:175–184.

Luo, X., I. Budihardjo, H. Zou, C. Slaughter, and X. Wang. 1998. Bid, a Bcl2 interacting protein, mediates cytochrome c release from mitochondria in response to activation of cell surface death receptors. *Cell.* 94:481–490.

MacFarlane, M., M. Ahmad, S.M. Srinivasula, T. Fernandes-Alnemri, G.M. Cohen, and E.S. Alnemri. 1997a. Identification and molecular cloning of two novel receptors for the cytotoxic ligand TRAIL. *J. Biol. Chem.* 272:25417–25420.

MacFarlane, M., K. Cain, X.-M. Sun, E.S. Alnemri, and G.M. Cohen. 1997b. Processing/activation of at least four interleukin-1β converting enzyme-like proteases occurs during the execution phase of apoptosis in human monocytic tumor cells. *J. Cell Biol.* 137:469–479.

Mancini, M., D.W. Nicholson, S. Roy, N.A. Thornberry, E.P. Peterson, L.A. Casciola-Rosen, and A. Rosen. 1998. The caspase-3 precursor has a cytosolic and mitochondrial distribution: implications for apoptotic signaling. *J. Cell Biol.* 140:1485–1495.

Moll, R., W.W. Franke, D.L. Schiller, B. Geiger, and R. Krepler. 1982. The catalogue of human cytokeratins: patterns of expression in normal epithelia, tumors and cultured cells. *Cell.* 31:11–24.

Muzio, M., A.M. Chinnaiyan, F.C. Kischkel, K. O'Rourke, A. Shevchenko, J. Ni, C. Scaffidi, J.D. Bretz, M. Zhang, R. Gentz, et al. 1996. FLICE, a novel FADD-homologous ICE/CED-3-like protease, is recruited to the CD95 (Fas/APO-1) death-inducing signalling complex. *Cell.* 85:817–827.

Pan, G., J. Ni, Y. Wei, G. Yu, R. Gentz, and V.M. Dixit. 1997. An antagonist decoy receptor and a death domain-containing receptor for TRAIL. *Science.* 277:815–818.

Prasad, S., V.A. Soldatenkov, G. Srinivasorao, and A. Dritschilo. 1998. Identification of keratins 18,19 and heat-shock protein 90β as candidate substrates of proteolysis during ionizing radiation-induced apoptosis of estrogen-receptor negative breast tumor cells. *Int. J. Oncology.* 13:757–764.

Rao, L., D. Perez, and E. White. 1996. Lamin proteolysis facilitates nuclear events during apoptosis. *J. Cell Biol.* 135:1441–1455.

Samali, A., B. Zhivotovsky, D.P. Jones, and S. Orrenius. 1998. Detection of pro-caspase-3 in cytosol and mitochondria of various tissues. *FEBS (Fed. Eur. Biochem. Soc.) Lett.* 431:167–169.

Scaffidi, C., J.P. Medema, P.H. Krammer, and M.E. Peter. 1997. Flice is predominantly expressed as two functionally active isoforms, caspase-8/a and caspase-8/b. *J. Biol. Chem.* 272:26953–26958.

Scaffidi, C., S. Fulda, A. Srinivasan, C. Friesen, F. Li, K.J. Tomaselli, K.-M. Debatin, P.H. Krammer, and M.E. Peter. 1998. Two CD95 (APO-1/Fas) signaling pathways. *EMBO (Eur. Mol. Biol. Organ.) J.* 17:1675–1687.

Sheridan, J.P., S.A. Marsters, R.M. Pitti, A. Gurney, M. Skubatch, D. Baldwin, L. Ramakrishnan, C.L. Gray, K. Baker, W.I. Wood, et al. 1997. Control of TRAIL-induced apoptosis by a family of signaling and decoy receptors. *Science*. 277:818–821.

Srinivasan, A., K.A. Roth, R.O. Sayers, K.S. Shindler, A.M. Wong, L.C. Fritz, and K.J. Tomaselli. 1998. In situ immunodetection of activated caspase-3 in apoptotic neurons in the developing nervous system. *Cell Death Differ*. 5:1004–1016.

Srinivasula, S.M., M. Ahmad, T. Fernandes-Alnemri, G. Litwack, and E.S. Alnemri. 1996. Molecular ordering of the Fas-apoptotic pathway: the Fas/APO-1 protease Mch5 is a CrmA-inhibitable protease that activates multiple Ced-3/ICE-like cysteine proteases. *Proc. Natl. Acad. Sci. USA*. 93:14486–14491.

Srinivasula, S.M., M. Ahmad, T. Fernandes-Alnemri, and E.S. Alnemri. 1998. Autoactivation of procaspase-9 by Apaf-1-mediated oligomerisation. *Mol. Cell.* 1:949–957.

Sun, X.-M., M. MacFarlane, J. Zhuang, B.B. Wolf, D.R. Green, and G.M. Cohen. 1999. Distinct caspase cascades are initiated in receptor-mediated and chemical-induced apoptosis. *J. Biol. Chem*. 274:5053–5060.

Takahashi, A., E.S. Alnemri, Y.A. Lazebnik, T. Fernandes-Alnemri, G. Litwack, R.D. Moir, R.D. Goldman, G.G. Poirier, S.H. Kaufmann, and W.C. Earnshaw. 1996. Cleavage of lamin A by Mch2α but not CPP32: multiple interleukin 1β-converting enzyme-related proteases with distinct substrate recognition properties are active in apoptosis. *Proc. Natl. Acad. Sci. USA*. 93:8395–8400.

Thornberry, N.A., and Y. Lazebnik. 1998. Caspases: enemies within. *Science.* 281:1312–1316.

van Engeland, M., H.J.H. Kuijpers, F.C.S. Ramaekers, C.P.M. Reutelingsperger, and B. Schutte. 1997. Plasma membrane alterations and cytoskeletal changes in apoptosis. *Exp. Cell Res.* 235:421–430.

Walczak, H., R.E. Miller, K. Ariail, B. Gliniak, T.S. Griffith, M. Jubin, W. Chin, J. Jones, A. Woodward, T. Le, et al. 1999. Tumoricidal activity of tumor necrosis factor-related apoptosis-inducing ligand in vivo. *Nat. Med.* 5:157–163.

Wang, K., X.-M. Yin, D.T. Chao, C.L. Milliman, and S.J. Korsmeyer. 1996. BID: a novel BH3 domain-only death agonist. *Genes Dev.* 10:2859–2869.

Woo, M., R. Hakem, M.S. Soengas, G.S. Duncan, A. Shahinian, D. Kägi, A. Hakem, M. McCurrach, W. Khoo, S.A. Kaufman, et al. 1998. Essential contribution of caspase 3/CPP32 to apoptosis and its associated nuclear changes. *Genes Dev.* 12:806–819.

Yin, X.-M., K. Wang, A. Gross, Y. Zhao, S. Zinkel, B. Klocke, K.A. Roth, and S.J. Korsmeyer. 1999. Bid-deficient mice are resistant to Fas-induced hepatocellular apoptosis. *Nature.* 400:886–891.

Zheng, T.S., S.F. Schlosser, T. Dao, R. Hingorani, I.N. Crispe, J.L. Boyer, and R.A. Flavell. 1998. Caspase-3 controls both cytoplasmic and nuclear events associated with Fas-mediated apoptosis in vivo. *Proc. Natl. Acad. Sci. USA*. 95:13618–13623.

Zhivotovsky, B., A. Samali, A. Gahm, and S. Orrenius. 1999. Caspases: their intracellular localization and translocation during apoptosis. *Cell Death Differ*. 6:644–651.